



**HAL**  
open science

## Neutralizing antibody levels as a correlate of protection against SARS-CoV-2 infection: a modeling analysis

Guillaume Lingas, Delphine Planas, H el ene P er e, Fran oise Porrot, Florence Guivel-Benhassine, Isabelle Staropoli, Darragh Duffy, Nicolas Chapuis, Camille Gobeaux, David Veyer, et al.

### ► To cite this version:

Guillaume Lingas, Delphine Planas, H el ene P er e, Fran oise Porrot, Florence Guivel-Benhassine, et al.. Neutralizing antibody levels as a correlate of protection against SARS-CoV-2 infection: a modeling analysis. *Clinical Pharmacology and Therapeutics*, 2024, 115 (1), pp.86-94. 10.1002/cpt.3069 . pasteur-04245549

**HAL Id: pasteur-04245549**

**<https://pasteur.hal.science/pasteur-04245549v1>**

Submitted on 17 Oct 2023

**HAL** is a multi-disciplinary open access archive for the deposit and dissemination of scientific research documents, whether they are published or not. The documents may come from teaching and research institutions in France or abroad, or from public or private research centers.

L'archive ouverte pluridisciplinaire **HAL**, est destin ee au d ep ot et  a la diffusion de documents scientifiques de niveau recherche, publi es ou non,  emanant des  tablissements d'enseignement et de recherche fran ais ou  trangers, des laboratoires publics ou priv es.



Distributed under a Creative Commons Attribution - NonCommercial 4.0 International License

Lingas Guillaume (Orcid ID: 0000-0001-8566-6220)  
 Schwartz Oliver (Orcid ID: 0000-0002-0729-1475)  
 Guedj Jeremie (Orcid ID: 0000-0002-5534-5482)

## Neutralizing antibody levels as a correlate of protection against SARS-CoV-2 infection: a modeling analysis

Guillaume Lingas<sup>1</sup>, Delphine Planas<sup>2,3</sup>, H el ene P er e<sup>4,5</sup>, Fran oise Porrot<sup>2</sup>, Florence Guivel-Benhassine<sup>2</sup>, Isabelle Staropoli<sup>2</sup>, Darragh Duffy<sup>6</sup>, Nicolas Chapuis<sup>7</sup>, Camille Gobeaux<sup>8</sup>, David Veyer<sup>4,5</sup>, Constance Delaugerre<sup>9,10</sup>, J er ome Le Goff<sup>9,11</sup>, Prunelle Getten<sup>12</sup>, J er ome Hadjadj<sup>13</sup>, Ad ele Bellino<sup>14</sup>, B eatrice Parfait<sup>15</sup>, Jean-Marc Treluyer<sup>16</sup>, Olivier Schwartz<sup>2,3</sup>, J er emie Guedj<sup>1,†</sup>, Solen Kern eis<sup>1,17,#</sup>, Benjamin Terrier<sup>18,19,#</sup>

<sup>1</sup> Universit e Paris Cit e, IAME, INSERM, F-75018, Paris ;

<sup>2</sup> Virus and Immunity Unit, Institut Pasteur, Universit e Paris Cit e, CNRS UMR3569, Paris, France.

<sup>3</sup> Vaccine Research Institute, Cr eteil, France.

<sup>4</sup> Microbiology Department, Virology Unit, APHP, H opital Europ een Georges-Pompidou, F-75015, Paris, France

<sup>5</sup> Universit e Paris Cit e, INSERM UMRS1138 Functional Genomics of Solid Tumors laboratory, F-75006, Paris, France

<sup>6</sup> Translational Immunology Unit, Institut Pasteur, Universit e Paris Cit e, Paris, France

<sup>7</sup> Assistance Publique-H opitaux de Paris. Centre-Universit e Paris Cit e, Service d'h ematologie biologique, H opital Cochin, Paris, France

<sup>8</sup> Department of automated biology, CHU de Cochin, AP-HP, Paris, France

<sup>9</sup> Virology Department, AP-HP, H opital Saint-Louis, F-75010 Paris, France

<sup>10</sup> Universit e Paris Cit e, Inserm U944, Biology of emerging viruses, F-75010, Paris, France

<sup>11</sup> Universit e Paris Cit e, Inserm U976, INSIGHT Team, F-75010, Paris, France

<sup>12</sup> INSERM UMRS 970, Universit e Paris Descartes, Paris, France.

<sup>13</sup> Department of Internal Medicine, National Reference Center for Rare Systemic Autoimmune Diseases, AP-HP, APHP.CUP, H opital Cochin, Paris, France.

<sup>14</sup> URC-CIC Paris Centre Necker/Cochin, AP-HP, H opital Cochin

<sup>15</sup> F ed eration des Centres de Ressources Biologiques - Plateformes de Ressources Biologiques AP-HP. Centre-Universit e Paris Cit e, Centre de Ressources Biologiques Cochin, H opital Cochin, F-75014, Paris, France

<sup>16</sup> Unit e de Recherche clinique, H opital Cochin, AP-HP. Centre - Universit e de Paris, Paris, France.

<sup>17</sup> Equipe de Pr evention du Risque Infectieux (EPRI), AP-HP, H opital Bichat, F-75018 Paris, France

<sup>18</sup> Department of Internal Medicine, National Reference Center for Rare Systemic Autoimmune Diseases, AP-HP, APHP.CUP, H opital Cochin, F-75014, Paris, France

<sup>19</sup> Universit e Paris Cit e, INSERM U970, Paris Cardiovascular Research Center, F-75015, Paris, France.

#These authors contributed equally to this work as co-senior authors.

† Corresponding author: [jeremie.guedj@inserm.fr](mailto:jeremie.guedj@inserm.fr)

### Conflict of interest statement :

H.P. received honoraria for lectures at MSD, JANSSEN, ViiV and SEEGENE. C.G. received payment for lectures and provision of study material from Roche Diagnostics, Nephrotek, Radiometer, and Siemens Healthineers; provision for study material from Hemcheck/Eurobio and participated on an Advisory Board for Siemens Healthineers and Gentian. C.D. received consulting fees from ViiV, Gilead and MSD. B.T. received consulting fees and honoraria for lectures from Vifor Pharma, AstraZeneca, GlaxoSmithKline and Pfizer. All other authors declared no competing interests for this work.

This article has been accepted for publication and undergone full peer review but has not been through the copyediting, typesetting, pagination and proofreading process which may lead to differences between this version and the [Version of Record](#). Please cite this article as doi: [10.1002/cpt.3069](https://doi.org/10.1002/cpt.3069)

**Funding:** The AMBU COV study was supported by the Fonds IMMUNOV, for Innovation in Immunopathology. An additional grant was obtained for immunological and virological experiments (COVID-19 grant number COV21039). The funding sources had no role in the study's design, conduct, and reporting.

## **Abstract**

While anti-SARS-CoV-2 antibody kinetics have been described in large populations of vaccinated individuals, we still poorly understand how they evolve during a natural infection and how this impacts viral clearance. For that purpose, we analyzed the kinetics of both viral load and neutralizing antibody levels in a prospective cohort of individuals during acute infection with alpha variant. Using a mathematical model, we show that the progressive increase in neutralizing antibodies leads to a shortening of the half-life of both infected cells and infectious viral particles. We estimated that the neutralizing activity reached 90% of its maximal level within 11 days after symptom onset and could reduce the half-life of both infected cells and circulating virus by a 6-fold factor, thus playing a key role to achieve rapid viral clearance. Using this model, we conducted a simulation study to predict in a more general context the protection conferred by pre-existing neutralization titers, due to either vaccination or prior infection. We predicted that a neutralizing activity, as measured by  $ED_{50} > 10^3$ , could reduce by 46% the risk of having viral load detectable by standard PCR assays and by 98% the risk of having viral load above the threshold of infectiousness. Our model shows that neutralizing activity could be used to define correlates of protection against infection and transmission.

## Study Highlights

o What is the current knowledge on the topic?

Antibody neutralization is associated to protection against symptomatic SARS-CoV-2 infection. However, it is unclear how it could be associated with protection against infection and transmission.

o What question did this study address?

This study aimed to establish a threshold for an immunological correlate of protection against SARS-CoV-2 infection and transmission

o What does this study add to our knowledge?

Neutralization titers decrease circulating virions and infected cells half-lives by 6 folds. Above  $10^3$  ED50 in patient's sera, our modeling predicts that viral replication could be dramatically reduced during an acute infection, reducing the risk of peak viral load being above the limit of detection by about 50% and the risk of being above the limit of infectiousness by about 98%.

o How might this change clinical pharmacology or translational science?

Our estimation of neutralizing activity required to reduce infection and transmission could be used to establish a threshold of protection and could guide future clinical studies.

## Introduction

The analysis of viral and immunological kinetics during severe acute respiratory coronavirus 2 (SARS-CoV-2) infection has provided important insights on some patterns of the virus, both at the individual (within-host) and population (between-host) levels. For instance, we and others have found that SARS-CoV-2 peak viral load was close or even coincided with the onset of symptoms, suggesting that identifying individuals before symptoms onset was key to efficiently reduce transmission<sup>1</sup>. Likewise, we and others identified that dynamics of viral load after the peak was associated with the risk of severe disease, and we used these predictions to quantify the clinical efficacy of antiviral strategies<sup>1,2</sup>. In addition, mathematical models of antibody kinetics after vaccination also played a key role to identify correlates of protection against symptomatic infection<sup>3</sup>.

A question that has remained largely unsolved is the impact of antibody kinetics on viral clearance, and how the induction of antibodies modulates the time to viral clearance. Because the virus constantly mutates, it has been shown in large observational studies that the measurement of total anti-Spike (S) IgG antibodies was important<sup>4-6</sup>, but that their neutralization capacity was also critical<sup>7</sup>. Neutralization titers ( $ED_{50}$ ; half-maximal effective dilution), provides a much more accurate description of the quantitative and qualitative level of protection of patients' sera, and can be used to compare the protection against different Variants of Concerns (VoC). This approach has been extensively used to analyze the magnitude and the duration of the protection conferred by mRNA vaccines<sup>8</sup>, and has played an important role to support booster dose strategies, or alert on the low level of protection of mRNA vaccine against disease acquisition in the Omicron variant era<sup>7,9</sup>.

However, the combined kinetic analysis of both viral dynamic and neutralizing activity has never been studied in detail in the context of an acute infection. Here, we relied on the AMBU COV cohort, a cohort of ambulatory individuals that took place in 2021 during the Alpha variant wave in France, prior to the mass vaccination campaign. Individuals were included

early after symptom onset, and both virological and immunological parameters were followed prospectively. We provided a detailed picture of the kinetics of antibody neutralization capacity against Alpha variant, but also against the VoC that emerged subsequently, including Delta and Omicron (BA.1) variants. Following previous studies in hospitalized patients<sup>1</sup>, we used mathematical modeling to characterize the impact of the kinetics of the neutralization activity on viral clearance. Then we used this model to predict how pre-existing neutralization activity conferred by natural infection or vaccination may reduce viral replication. We put these results in perspective to discuss the efficacy of vaccines and more broadly the use of neutralizing titers as a correlate of protection against infection and transmission.

## **Patients and methods**

### ***Study design***

The AMBU COV study (APHP201285, N° IDRCB /EUDRACT: 2020-A03102-37, ClinicalTrial.gov: NCT04703114) is a non-interventional longitudinal study that included 57 individuals between 05 February 2021 and 20 May 2021 in Cochin Hospital (Paris, France). The AMBU COV study was an ancillary study of the cross-sectional SALICOV study (NCT04578509), that aimed to compare diagnostic accuracy of two alternate diagnosis strategies (nasopharyngeal antigen test and saliva nucleic acid amplification testing) to the current reference standard (nasopharyngeal nucleic acid amplification testing) for detection of SARS-CoV-2 in community testing centers<sup>10</sup>. The SALICOV study was conducted in the network of community screening centers of the Assistance Publique-Hôpitaux de Paris (APHP), France. Briefly, all individuals with symptoms (i.e., temperature > 37.8 °C or chills, cough, rhinorrhea, muscle pain, loss of smell or taste, unusual persistent headaches, or severe asthenia) were invited to be tested for SARS-CoV-2 in two community screening centers located in Paris. Testing was also available to all asymptomatic individuals wishing to be tested (i.e., contact of infected cases, before or after travel, after participation to a gathering

event). Once their participation to SALICOV was completed, participants tested positive for SARS CoV-2 were contacted by phone by the principal investigator (BT) to explain the study protocol and offered to participate in the AMBU COV study. Home visits were organized and written informed consent was obtained from all included participants (or their legal representatives if unable to consent).

Exclusion criteria included patients with criteria for hospitalization at the time of diagnosis, non-consent or inability to obtain consent, patients with dementia or not authorized, for psychiatric reasons or intellectual failure, to receive information on the protocol and to give informed consent, and patients under guardianship or curatorship.

### ***Study population and procedures***

All adults included in the SALICOV study, with a positive nasopharyngeal PCR for SARS-CoV-2 within 48 hours, either with or without symptoms were included in the AMBU COV study.

For each participant, four home visits were done by study nurses on day 0 (defined as the first study visit), day 3, day 8 and day 15. Blood samples were collected at each home visit, saliva on day 3, day 8 and day 15, nasal swab on day 8 and day 15 and stools on day 3 and day 15.

A follow-up study was performed at Cochin Hospital (Paris, France) on day 90 to collect outcome data and additional biological samples (blood, saliva and stools). Saliva samples were self-collected under supervision of the nurse or the principal investigator. Blood samples, saliva and stools samples were centralized, frozen in several aliquots at  $-80^{\circ}\text{C}$  within 24 hours and stored for analysis.

### ***Data collection***

We collected data on sociodemographic, past medical history, presence of symptoms and concomitant medications using a standardized data collection form.

### ***Role of the funding sources***

The AMBU COV study was supported by the Fonds IMMUNOV, for Innovation in Immunopathology. An additional grant was obtained for immunological and virological experiments (COVID-19 grant number COV21039). The funding sources had no role in the study's design, conduct, and reporting.

### ***Institutional Review Board (IRB) approval***

The IRB C.P.P. Ile de France III approved the study protocol prior to data collection (approval number Am8849-2-3853-RM) and all subsequent amendments.

### ***Quantification of SARS-CoV2 RNA in saliva samples***

Viral RNA was extracted from saliva samples using the Cellfree200 V7 DSP 200 protocol with the QIA Symphony® DSP virus/pathogen mini kit (QIAGEN, UK). Samples loaded onto the QIA Symphony® SP as instructed by the manufacturer, with a 200 µl sample input volume and 60 µl elution output volume of AVE buffer, unless stated (QIAGEN, UK). SARS-CoV-2 RT-ddPCR assays were performed using the One-Step RT-ddPCR Advanced Kit for 90 Probes (Bio-Rad Laboratories, Hercules, CA, USA) and the QX200 ddPCR platform (Biorad). A 2-plex RT-ddPCR assay was developed, which targets the Nucleocapside (N1) gene of the SARS-CoV-2 positive-strand RNA genome with specific FAM- probe and primers Cy5-labeled probe for the detection of a human housekeeping gene (RNaseP). RNaseP positivity was necessary to validate the RT-PCR assay prior to any further analysis. We considered 6 log<sub>10</sub> copies/mL as a proxy for positive viral culture<sup>1</sup>.

### ***S-Flow Assay***

The S-Flow assay is based on the recognition of the SARS-CoV-2 spike protein expressed on the surface of 293T cells. It was used to quantify SARS-CoV-2-specific IgG and IgA subtypes in sera as previously described<sup>11,12</sup>. Briefly, 293T cells were obtained from ATCC (ATCC Cat# CRL-3216, RRID:CVCL\_0063) and tested negative for mycoplasma. 293T cells stably expressing Spike (293T S) or control (293T Empty) were transferred into U-bottom 96-well

plates ( $10^5$  cells/well). Cells were incubated at 4°C for 30 min with serum (1:300 dilution), saliva (1:5 dilution) or nasopharyngeal swabs (1:5 dilution) in PBS containing 0.5% BSA and 2 mM EDTA. Then, cells were washed with PBS, and stained at 4°C for 30 min using anti-IgG AlexaFluor647 (Jackson ImmunoResearch cat# 109-605-170) and Anti-IgA AlexaFluor488 (Jackson ImmunoResearch cat# 109-545-011). Then, cells were washed with PBS and fixed 10 min with 4% PFA. Data were acquired on an Attune Nxt instrument (Life Technologies). Results were analyzed with FlowJo 10.7.1 (Becton Dickinson). The specific binding was calculated as follow:  $100 \times (\% \text{ binding } 293\text{T Spike} - \% \text{ binding } 293\text{T Empty}) / (100 - \% \text{ binding } 293\text{T Empty})$ . For sera, the assay was standardized with WHO international reference sera (20/136 and 20/130) and cross-validated with two commercially available ELISA (Abbott and Beckmann) using a Passing-Bablok linear regression model to allow calculation of BAU/mL<sup>13</sup>. SARS-CoV-2 neutralization was assessed using the S-fuse assay, as previously described<sup>14</sup>.

#### ***S-Fuse neutralization assay***

U2OS-ACE2 GFP1-10 or GFP 11 cells, also termed S-Fuse cells, become GFP+ when they are productively infected by SARS-CoV-2<sup>15</sup>. Cells tested negative for mycoplasma. Cells were mixed (ratio 1:1) and plated at  $8 \times 10^3$  per well in a  $\mu$ Clear 96-well plate (Greiner Bio-One). The indicated SARS-CoV-2 strains were incubated with serially diluted sera for 15 min at room temperature and added to S-Fuse cells. Sera were heat-inactivated for 30 min at 56 °C before use. 18 h later, cells were fixed with 2% PFA, washed and stained with Hoechst (dilution of 1:1,000, Invitrogen). Images were acquired using an Opera Phenix high-content confocal microscope (PerkinElmer). The GFP area and the number of nuclei were quantified using the Harmony software (PerkinElmer). The percentage of neutralization was calculated using the number of syncytia as value with the following formula:  $100 \times (1 - (\text{value with serum} - \text{value in 'non-infected'}) / (\text{value in 'no serum'} - \text{value in 'non-infected'}))$ . Neutralizing activity of each serum was expressed as the half maximal effective dilution (ED<sub>50</sub>).

## Viral strain

B.1.1.7 (Alpha variant) was isolated from an individual in Tours (France) who had returned from the UK (PMID: 33772244). B.1.617.2 (Delta variant) was isolated from a nasopharyngeal swab of a hospitalized patient who had returned from India. The swab was provided and sequenced by the Laboratoire de Virologie of the Hôpital Européen Georges Pompidou (Assistance Publique des Hôpitaux de Paris) (PMID: 34237773). The Omicron BA.1 strain was supplied and sequenced by the NRC UZ/KU Leuven (Leuven, Belgium) (PMID: 35016199). All individuals provided informed consent for the use of the biological materials. The variant strains were isolated from nasal swabs on Vero cells and amplified by one or two passages on Vero cells.

Titration of viral stocks was performed on Vero E6, with a limiting dilution technique allowing a calculation of TCID<sub>50</sub>, or on S-Fuse cells. Viruses were sequenced directly on nasal swabs, and after one or two passages on Vero cells. Sequences were deposited in the GISAID database immediately after their generation, with the following IDs: Alpha: EPI\_ISL\_735391; Delta: ID: EPI\_ISL\_2029113; Omicron BA.1.

### **Model for antibody and ED<sub>50</sub> kinetics**

We modeled the evolution of IgG levels using a sigmoid Gompertz function<sup>16</sup> to reflect the progressive increase in IgG from 0 (before infection) to a plateau, noted IgG<sub>max</sub>, with dimensionless parameters A and B driving the equation:

$$\text{IgG}(t) = \text{IgG}_{\text{max}} \times e^{-e^{-(A-B \times t)}}$$

We next relate IgG to the evolution of the neutralizing activity (ED<sub>50</sub>) against different strains, namely Alpha ( $\alpha$ ), Delta ( $\delta$ ) and Omicron (BA.1,  $\omicron$ ) using the following relationship:

$$\begin{aligned} \text{ED}_{50}^{\alpha}(t) &= \zeta \times \text{IgG}(t) \\ \text{ED}_{50}^{\delta}(t) &= f_{\delta} \times \zeta \times \text{IgG}(t) \\ \text{ED}_{50}^{\omicron}(t) &= f_{\omicron} \times \zeta \times \text{IgG}(t) \end{aligned}$$

such that  $\zeta$  represents the scaling factor between IgG and ED<sub>50</sub> <sup>$\alpha$</sup> , while  $f_{\delta}$  (resp  $f_{\omicron}$ ) represent the fold change between the neutralization capacity against delta variant (resp. omicron). Of

note, in this model, the time to reach 90% of the maximal protection is the same for all variants and is equal to  $(A - \log(-\log(0.9)))/B$ .

### **Model for viral dynamics in saliva**

We used a target-cell limited model with an eclipse phase as described before<sup>1</sup> (**Figure S1**) to characterize viral dynamics in saliva from infection ( $t=0$ ) to clearance. In brief, the model includes three types of cell populations: target cells ( $T$ ), infected cells in an eclipse phase ( $I_1$ ) and productively infected cells ( $I_2$ ). The model assumes that target cells are infected at a constant infection rate  $\beta$  ( $\text{mL.virion}^{-1}.\text{d}^{-1}$ ). Once infected, cells enter an eclipse phase and become productively infected after a mean time  $1/k$  (day). We assume that productively infected cells have a constant loss rate, noted  $\delta$  ( $\text{d}^{-1}$ ). Infected cells produce  $p$  viral particles per day ( $\text{virus}.\text{d}^{-1}$ ), but only a fraction of them,  $\mu$ , is infectious, and the virus particles can either be infectious ( $V_i$ ) or non-infectious ( $V_{NI}$ ). We assumed that viral load, as measured by RNA copies ( $V$ ), is the sum of infectious and non-infectious viral particles, both cleared at the same rate,  $c$ . The model can be written as :

$$\begin{aligned}\frac{dT}{dt} &= -\beta V_i T \\ \frac{dI_1}{dt} &= \beta V_i T - k I_1 \\ \frac{dI_2}{dt} &= k I_1 - \delta I_2\end{aligned}\tag{Eq. 1}$$

$$\begin{aligned}\frac{dV_i}{dt} &= p \mu I_2 - c V_i \\ \frac{dV_{ni}}{dt} &= p(1 - \mu) I_2 - c V_{NI}\end{aligned}$$

The basic reproductive number  $R_0$ , defined by the number of secondary infected cells resulting from one infected cell in a population of fully susceptible cells,  $T_0$ , is defined by :

$$R_0 = \frac{\beta p T_0 \mu}{c \delta}$$

### **Combined immunovirological model**

Finally, we aimed to characterize the impact of the neutralizing antibody level on viral load. For that purpose, we tested several models, assuming no effect of neutralization antibody levels (model M0, Eq. 1), or that the effect of neutralization could alternatively i) increase infected cell clearance (model M1), ii) increase the loss of both infectious and non-infectious virus (model M2), iii), both (model M3) or both with the same efficacy (model M4) (**Figure S1**).

Model M0:

$$\frac{dI_2}{dt} = kI_1 - \delta I_2, \frac{dV_I}{dt} = p\mu I_2 - cV_I, \frac{dV_{NI}}{dt} = p(1 - \mu)I_2 - cV_{NI}$$

Model M1:

$$\frac{dI_2}{dt} = kI_1 - I_2\delta[1 + \varphi_\delta \log_{10}(1 + ED_{50}^\alpha)], \frac{dV_I}{dt} = p\mu I_2 - cV_I, \frac{dV_{NI}}{dt} = p(1 - \mu)I_2 - cV_{NI}$$

Model M2

$$\frac{dI_2}{dt} = kI_1 - \delta I_2, \frac{dV_I}{dt} = p\mu I_2 - V_I c[1 + \varphi_c \log_{10}(1 + ED_{50}^\alpha)], \frac{dV_{NI}}{dt} = p(1 - \mu)I_2 - V_{NI} c[1 + \varphi_c \log_{10}(1 + ED_{50}^\alpha)]$$

Model M3:

$$\frac{dI_2}{dt} = kI_1 - I_2\delta[1 + \varphi_\delta \log_{10}(1 + ED_{50}^\alpha)], \frac{dV_I}{dt} = p\mu I_2 - V_I c[1 + \varphi_c \log_{10}(1 + ED_{50}^\alpha)],$$

$$\frac{dV_{NI}}{dt} = p(1 - \mu)I_2 - V_{NI} c[1 + \varphi_c \log_{10}(1 + ED_{50}^\alpha)]$$

Model M4:

$$\frac{dI_2}{dt} = kI_1 - I_2[\delta + \varphi \log_{10}(1 + ED_{50}^\alpha)], \frac{dV_I}{dt} = p\mu I_2 - V_I c[1 + \varphi \log_{10}(1 + ED_{50}^\alpha)], \frac{dV_{NI}}{dt} =$$

$$p(1 - \mu)I_2 - V_{NI} c[1 + \varphi \log_{10}(1 + ED_{50}^\alpha)]$$

**Assumptions on parameter values**

We fixed  $c$  to  $10 \text{ d}^{-1}$ ,  $k$  to  $4 \text{ d}^{-1}$  and  $\mu$  to  $10^{-4}$  as previously published<sup>1</sup>. As only the product  $p \times T_0$  is identifiable, we also fixed the density of susceptible epithelial cells to the same value found in the upper respiratory tract, i.e.,  $T_0 = 1.33 \times 10^5 \text{ cells.mL}^{-1}$ . Further we assumed that the duration of the incubation period was log-normally distributed, with a median value of 5 days a standard deviation of 0.125, such that 90% of individuals have an incubation period between 3 and 7 days<sup>1</sup>. Thus, only 3 viral parameters were estimated, namely  $p$ ,  $\delta$  and  $R_0$ , along with their interindividual variabilities. Given the lack of data on the viral upslope, we also fixed the standard deviation of the random effect associated to  $R_0$ , denoted  $\omega_{R_0}$  to 0.5, as done previously<sup>1</sup>.

### ***Inference & model selection***

Models M0, M1, M2, M3 and M4 were fitted to all data available, namely viral load, IgG and  $ED_{50}$  against all strains, assuming an additive error on the log-quantities. Parameters were estimated using non-linear mixed effect models and SAEM algorithm, using the same statistical methodology as previously described<sup>1,17</sup>. Only the results obtained with the best model are presented.

### ***Impact of a pre-existing neutralization capacity on viral dynamics***

Next, we used the best model to anticipate the viral dynamics that could be observed in non-naive individuals, i.e., in individuals having a pre-existing neutralization due either natural infection or vaccination. For that purpose, we assumed that one virus was present at  $t=0$  (infection time), and we assumed different levels of neutralizing capacity ranging from  $ED_{50}=0$  to  $ED_{50}=10^5$ . For each value of  $ED_{50}$  we generated a large population of 5,000 virological profiles using the final immuno-virological model, and we calculated different viral metrics. Of note, we made the conservative assumption here that the neutralizing capacity remained constant during the infection, i.e., we did not consider any increase over time due to stimulated immune response. As a sensitivity analysis, we also calculated the protection obtained with the alternative models.

## **Results**

### ***Baseline characteristics***

A total of 57 patients were included between February and September 2021 (**Table 1**). Patients were mostly male ( $N=40$ , 63%), with a median age of 44 years (IQR: 35-57) and all were infected with the Alpha variant. Fifty-five participants developed symptoms, and 2 remained asymptomatic throughout the study. Patients had very few comorbidities, and hypertension (5%), chronic cardiac disease (5%), obesity (3%), and chronic kidney disease (2%) were the most common comorbidities. One patient was fully vaccinated (2 doses) and 7 patients had received one dose of vaccination at the time of infection. The median time between symptoms onset and inclusion in the AMBU COV study was 4 (IQR: 3-6) days and the median saliva viral load at inclusion was 6.27 (IQR: 5.61-6.93)  $\log_{10}$  copies/mL.

### ***Immuno-virological modeling***

All data used for the modeling exercise, namely viral load (in saliva), anti-S IgG and neutralizing titers (in plasma or serum) are shown in **Figure 1** and **Figure S2**.

The model best describing our data assumed that neutralizing antibodies acted on both infected cell and infectious virus clearance with the same efficacy (Model M4), and the model could well fit all data (**Figure 2, Figure S3 & S4, Tables S1-4**). Model parameters were in line with what we found in other studies, with a within-host  $R_0$  equal to 29.6, a viral production rate of  $2.91 \times 10^3$  viruses/cell/day, and a loss rate of infected cells in absence of antibodies equal to  $\delta = 0.23 \text{ d}^{-1}$  (**Table S4**). The peak viral load occurred at symptom onset with a median level of 6.7  $\log_{10}$  RNA copies/mL.

The population average maximal level of anti-S IgG after acute infection,  $\text{IgG}_{\text{max}}$ , was equal to 152 BAU/mL, corresponding to an antibody neutralization level against  $\alpha$  variant,  $\zeta^* \text{IgG}_{\text{max}}$ ,

equal to 541 ED<sub>50</sub>. This level was achieved progressively after infection, and we predicted that 90% of this maximal antibody protection was achieved 10.6 days after symptom onset. This level of neutralization was achieved around day 6 after symptoms onset in patients vaccinated with one dose, and the only patient that had received 2 doses at the time of the infection reached this level only 4 days after symptoms onset, supporting that vaccination considerably reduced the time to achieve high level of neutralization activity. At antibody peak, we estimated that the half-lives of both infected cells and infectious virus were shortened by 6 fold (corresponding to loss rates for  $\delta$  and  $c$  equals to 1.31 d<sup>-1</sup> and 57.30 d<sup>-1</sup>, respectively). Because antibody levels reached their maximal value after peak viral load, we did not find a significant association between the cumulated levels of neutralizing antibody levels and viral load (**Figure S5**). As all individuals were infected with Alpha variant, the population average maximal level of neutralization against Delta and BA.1 variants were much lower and were diminished by respectively 6.7- and 266.7-folds, leading to median ED<sub>50</sub> of 81 and 2, respectively, after infection, reached around 10 days after symptom onset.

To address the impact of the temporal effect of antibody levels on viral clearance, we simulated 5,000 *in silico* virological profiles using the estimated parameter distributions and considering that antibody could have either the two mechanisms of action (as found in our model), only one of them or none of them (thus fixing alternatively  $\varphi_\delta$  and/or  $\varphi_c$  to 0 in the model). When considering the full model, the predicted median time to clearance after symptoms onset was equal to 12 days, as compared to >50 in a model in which antibodies had no effect ( $\varphi = 0$ ). We observed that the effectiveness of IgG was predominantly driven by its action on the loss rate of infected cells, with a median time to viral clearance equal to 14 days when only the effects on infected cell was assumed ( $\varphi_c = 0$ ) as compared to >50 days when only the effects on infected viral particles was assumed ( $\varphi_\delta = 0$ ) (**Figure S6**). Consistent with this prediction, the post-hoc analysis showed that the early appearance of detectable neutralizing antibodies was associated with lower viral levels at day 4 post-symptom onset, which corresponds to the median time of inclusion in the study ( $r=0.46$ , ( $P<10^{-3}$ , **Figure S5**).

### ***Impact of a pre-existing neutralization capacity on viral dynamics***

Next, we used the model to anticipate the viral dynamics that could be observed after infection of a non-naive individual having a pre-existing neutralization, due either natural infection or vaccination. For that purpose, we assumed that infection is initiated at  $t=0$  with only one infectious particle, and we assumed different levels of neutralizing capacity ranging from  $ED_{50}=0$  to  $ED_{50}=10^5$  (see methods). This corresponds to a within-host  $R_0$  ranging from 29.6 (i.e., the value estimated in our population before antibody secretion) to about 0.7. Using the model parameters, we simulated viral dynamics of 5,000 individuals with each potential level of  $ED_{50}$  and we computed the following metrics: peak viral load, probability of having detectable viral load at peak, probability of having viral load  $> 6 \log_{10}$  copies/mL. The simulations showed that  $ED_{50}>10^3$  would be sufficient to maintain 45% of individuals with viral load below the limit of detection at all times and 98% of individuals below the threshold of infectiousness (i.e., peak viral load above  $> 6 \log_{10}$  copies/mL, Figure 3, Table 2) at all times.

## Discussion

In this work, we combined the kinetic analysis of saliva viral load and immune response during acute SARS-CoV-2 Alpha strain infection in ambulatory patients with non-severe disease. We showed that neutralizing antibodies played a key role to achieve rapid viral clearance by reducing the half-life of both infected cells and viral particles. The neutralizing activity was largely variant-dependent, and ED<sub>50</sub> was estimated to 541 against Alpha variant but decreased by 6.7- and 266-folds against Delta and Omicron BA.1 variants, respectively. We performed simulations to predict the level of protection against infection assuming different levels of antibody neutralization. We predicted that a level of ED<sub>50</sub> > 10<sup>3</sup> could reduce the risk of infection by 50% (as measured by the probability of peak viral load being above the limit of detection by standard PCR) and the risk of infectiousness by 98% (as measured by the probability of peak viral load above 10<sup>6</sup> copies/mL). Overall, this value of neutralizing activity could therefore be used to identify individuals with poor protection against infection and transmission of the virus.

Our study has several limitations. First the model follows the interplay between viral and antibody kinetics, but the two quantities were not measured in the same compartment, the first being obtained in saliva and the second in serum, respectively. Although the antibody level measured in the serum is likely a good reflect of the concentration in other compartments, it is possible that the kinetics may differ, due for instance to different levels of viral replication over time, as observed for saliva and nasopharynx for instance<sup>18</sup>. This could induce a bias in the relationship found here between the neutralizing activity and the viral load. Second, as it is the case in such studies, very few data could be measured before symptom onset and peak viral load, which may hamper the estimation of both viral kinetic parameters and the corresponding effects of neutralization, as discussed previously<sup>1,18</sup>. Overcoming this issue requires specific study designs that identify individuals before symptom onset, and ideally immediately after infection, for instance via repeated PCR-testing policy in uninfected individuals. Further, we only modeled antibody kinetics and no measurements of the T-cell

Accepted Article

response was available. We made the conservative assumption that the kinetics of antibody could solely explain viral clearance, recognizing that this premise may not hold true, as T-cell are both associated with viral clearance<sup>19</sup> and protection against infection<sup>20</sup>. Also, we relied on peak viral load as a proxy for infection. This may therefore overestimate the level of neutralizing activity that could be observed in real conditions, as infection detection largely depends on the presence of symptoms, which was not modeled here and could depend on the level of viral replication (note that the latter is controversial and was not observed in human challenge study<sup>21</sup>).

We conducted a formal identifiability analysis to evaluate the precision of estimation that could be expected given the data limitation discussed above. We found that the effect of neutralization could be precisely identified here (**Table S6**). To evaluate the sensitivity of our results to the identified mechanisms of action, we conducted simulations using a model where antibodies would only act on the loss rate of infected cells (model M1). We found that the resulting protection conferred by any level of ED<sub>50</sub> was much lower, with proportion of detectable individuals at peak viral load being >98% at all concentrations (Figure & Table S7).

Interestingly, the threshold found in our study can be compared with findings from other studies. In a cohort of vaccinated elderly individuals prospectively followed during the Omicron BA.1 wave, it was found that individuals that were infected had much lower levels of neutralization than those that remained uninfected, with median levels of 281 and 1376, respectively, and no infection reported in individuals with ED<sub>50</sub> larger than 2136<sup>22</sup>. In another study, patients infected with Alpha variant exhibited a median level of protection of 108 ED<sub>50</sub> one month prior to infection, compared to 2483 ED<sub>50</sub> for uninfected patients<sup>8</sup>. Finally, an important question is probably whether such levels can be achieved after vaccination. In a prospective study of uninfected, mostly young individuals that received mRNA vaccine, we showed that vaccination with Bnt162b2 could lead to high levels of neutralizing activity for some period of time against pre-omicron variants, but not against any of the omicron variants<sup>23</sup>. This confirms that vaccination with Bnt162b2, although it maintains high level of

Accepted Article

protection against severe disease, has limited activity against infection and transmission with Omicron viruses. Whether such levels can be attained with bivalent vaccines may therefore be key to reduce virus circulation in the future. These results can also be compared to results obtained in other population with other assays by normalizing with the level of neutralization achieved after infection. Our threshold of  $10^3$  ED<sub>50</sub> to prevent infection and transmission corresponds to about 2-folds the peak neutralization value achieved after infection (Fig 2). Other studies<sup>3,24</sup> have shown that a 50% protection against symptomatic disease was achieved with a level of neutralization equivalent to 20% of the mean human convalescent titers. This, therefore, confirms that the level of protection required to prevent infection and transmission is much larger than what is required to prevent symptomatic infection.

Our proposed correlate of protection could be validated in prospective studies by following a large cohort of uninfected individuals where both plasma and possibly nasopharyngeal viral load would be regularly sampled to document infection. Validating a threshold against transmission is more complex and would require to follow infected individuals and their contacts. One ideal framework could be to focus on specific settings, such as households where both index cases and their contacts can be followed to measure the viro-immunological response.

In conclusion, our data show that ED<sub>50</sub> >  $10^3$  could be a clinically relevant threshold value for the neutralizing activity to identify individuals with poor protection against infection and higher risk of transmission. The evaluation of this threshold on larger cohorts is now warranted to evaluate whether it could be used to define a correlate of protection against infection and transmission.

**Authors contribution:**

G.L., D.P., B.T., S.K., and J.G. wrote the manuscript. J.G., B.T., and S.K. designed the research. G.L., D.P., B.T., S.K., J.G., H.P., F.P., F.G-B., I.S., D.D, N.C., C.G., D.V., C.D., J.LG., P.G., J.H., A.B., B.P., J-M.T., and O.S., performed the research, G.L. and J.G. analyzed the data.

## References

1. Néant, N. *et al.* Modeling SARS-CoV-2 viral kinetics and association with mortality in hospitalized patients from the French COVID cohort. *Proc Natl Acad Sci U S A* **118**, e2017962118 (2021).
2. Ke, R., Zitzmann, C., Ho, D. D., Ribeiro, R. M. & Perelson, A. S. In vivo kinetics of SARS-CoV-2 infection and its relationship with a person's infectiousness. *Proc Natl Acad Sci U S A* **118**, (2021).
3. Khoury, D. S. *et al.* Neutralizing antibody levels are highly predictive of immune protection from symptomatic SARS-CoV-2 infection. *Nat Med* **27**, 1205–1211 (2021).
4. Chivu-economescu, M. *et al.* Assessment of the Humoral Immune Response Following COVID-19 Vaccination in Healthcare Workers: A One Year Longitudinal Study. *Biomedicines* **2022**, Vol. 10, Page 1526 **10**, 1526 (2022).
5. Chiara, C. Di *et al.* Long-term Immune Response to SARS-CoV-2 Infection Among Children and Adults After Mild Infection. *JAMA Netw Open* **5**, e2221616–e2221616 (2022).
6. Sasso, B. Lo *et al.* Longitudinal analysis of anti-SARS-CoV-2 S-RBD IgG antibodies before and after the third dose of the BNT162b2 vaccine. *Scientific Reports* **2022** **12**:1 **12**, 1–7 (2022).
7. Planas, D. *et al.* Considerable escape of SARS-CoV-2 Omicron to antibody neutralization. *Nature* **2021** **602**:7898 **602**, 671–675 (2021).
8. Bruel, T. *et al.* Neutralising antibody responses to SARS-CoV-2 omicron among elderly nursing home residents following a booster dose of BNT162b2 vaccine: A community-based, prospective, longitudinal cohort study. *EClinicalMedicine* **51**, 101576 (2022).
9. Bruel, T. *et al.* Serum neutralization of SARS-CoV-2 Omicron sublineages BA.1 and BA.2 in patients receiving monoclonal antibodies. *Nature Medicine* **2022** **28**:6 **28**, 1297–1302 (2022).
10. Kernéis, S. *et al.* Accuracy of saliva and nasopharyngeal sampling for detection of SARS-CoV-2 in community screening: a multicentric cohort study. *European Journal of Clinical Microbiology and Infectious Diseases* **40**, 2379–2388 (2021).
11. Grzelak, L. *et al.* A comparison of four serological assays for detecting anti-SARS-CoV-2 antibodies in human serum samples from different populations. *Sci Transl Med* **12**, 3103 (2020).
12. Grzelak, L. *et al.* Sex Differences in the Evolution of Neutralizing Antibodies to Severe Acute Respiratory Syndrome Coronavirus 2. *J Infect Dis* **224**, 983–988 (2021).
13. Hadjadj, J. *et al.* Immunogenicity of BNT162b2 vaccine against the Alpha and Delta variants in immunocompromised patients with systemic inflammatory diseases. *Ann Rheum Dis* **81**, 720–728 (2022).
14. Planas, D. *et al.* Sensitivity of infectious SARS-CoV-2 B.1.1.7 and B.1.351 variants to neutralizing antibodies. *Nat Med* **27**, 917–924 (2021).
15. Buchrieser, J. *et al.* Syncytia formation by SARS-CoV-2-infected cells. *EMBO J* **39**, (2020).
16. Tjørve, K. M. C. & Tjørve, E. The use of Gompertz models in growth analyses, and new Gompertz-model approach: An addition to the Unified-Richards family. *PLoS One* **12**, e0178691 (2017).

17. Gonçalves, A. *et al.* Timing of Antiviral Treatment Initiation is Critical to Reduce SARS-CoV-2 Viral Load. *CPT Pharmacometrics Syst Pharmacol* **9**, 509–514 (2020).
18. Ke, R. *et al.* Daily longitudinal sampling of SARS-CoV-2 infection reveals substantial heterogeneity in infectiousness. *Nature Microbiology* **2022 7:5 7**, 640–652 (2022).
19. Helen Wagstaffe, A. R. *et al.* Mucosal and Systemic Immune Correlates of Viral Control following SARS-CoV-2 Infection Challenge in Seronegative Adults. *medRxiv* 2023.07.21.23292994 (2023).doi:10.1101/2023.07.21.23292994
20. Chandrashekar, A. *et al.* SARS-CoV-2 infection protects against rechallenge in rhesus macaques. *Science (1979)* **369**, 812–817 (2020).
21. Killingley, B. *et al.* Safety, tolerability and viral kinetics during SARS-CoV-2 human challenge in young adults. *Nature Medicine* **2022 28:5 28**, 1031–1041 (2022).
22. Boudhabhay, I. *et al.* COVID-19 outbreak in vaccinated patients from a haemodialysis unit: antibody titres as a marker of protection from infection. *Nephrology Dialysis Transplantation* **37**, 1357–1365 (2022).
23. Clairon, Q. *et al.* Modeling the kinetics of the neutralizing antibody response against SARS-CoV-2 variants after several administrations of Bnt162b2. *PLoS Comput Biol* **19**, e1011282 (2023).
24. Kandala, B. *et al.* Accelerating model-informed decisions for COVID-19 vaccine candidates using a model-based meta-analysis approach. *EBioMedicine* **84**, 104264 (2022).

# Tables and figures

	Median/N (IQR/%)
Age (years)	43 (33-54)
BMI (kg/m <sup>2</sup> )	23.9 (21.3-25.3)
Male Gender	36 (63%)
At least 1 comorbidity*	6 (11%)
Delay between symptom onset and inclusion	4 (3-6)
Vaccinated (1 dose)	7 (12%)
Vaccinated (2 doses)	1 (2%)
IgG (log <sub>10</sub> BAU/mL of serum)	0.5 (3-1.2)
Saliva viral load (log <sub>10</sub> copies/mL)	6.4 (5.74-6.93)
Log <sub>10</sub> ED <sub>50</sub> <sup>α</sup>	2.6 (2.1-3.5)
Log <sub>10</sub> ED <sub>50</sub> <sup>δ</sup>	2.1 (1.2-2.6)
Log <sub>10</sub> ED <sub>50</sub> <sup>o</sup>	LOQ

\*Hypertension, Obesity, Heart failure or Kidney failure

**Table 1. Clinical and biological characteristics at inclusion in the AMBU COV study.**

Antibody neutralization level at infection (ED <sub>50</sub> )	Fold change relative to mean estimated peak ED <sub>50</sub>	Median peak viral load (log <sub>10</sub> copies/mL)	Probability of peak viral load above the limit of detection	Probability of peak viral load above the threshold of infectivity
0	NA	7.2	100%	80%
10 <sup>1</sup>	0.02	6.0	99%	48%
10 <sup>2</sup>	0.2	4.1	85%	14%
10 <sup>3</sup>	2	1.9	54%	2%
10 <sup>4</sup>	20	1.7	40%	0%
10 <sup>5</sup>	200	1.6	33%	0%

**Table 2. Predicted impact of a pre-existing antibody neutralization on viral kinetics. The limit of detection and the threshold of infectivity were set to 1.84 and 6 log<sub>10</sub> copies/mL, respectively.**

## FIGURE LEGEND

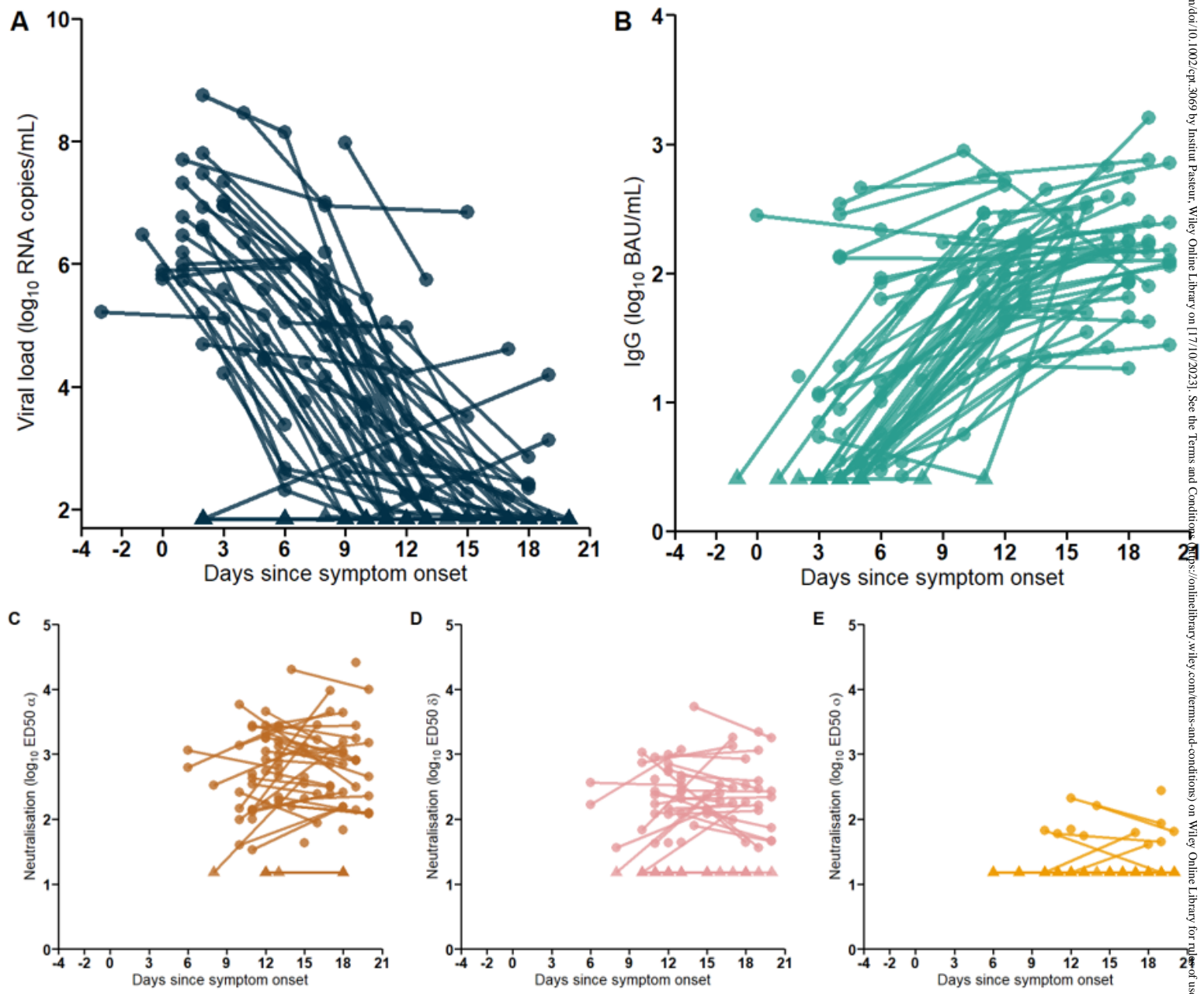
**Figure 1. Virological and immunological data analyzed in the AMBU COV cohort.** A. Saliva viral load. B. Serum concentration of IgG (BAU/mL). C-E. Neutralization activity of IgG against strains C. Alpha D. Delta. E. Omicron (BA.1). All data expressed in time since symptom onset. Triangles represent data below LOQ.

**Figure 2. Median predictions of viral (A) and serological (B) kinetics.** Circles are the observed data and lines represent the simulation-based median predictions of the model. Triangles represent data below LOQ. Darkblue: Viral load. Lightblue: IgG. Brown: ED<sub>50</sub>α. Pink: ED<sub>50</sub>δ. Yellow: ED<sub>50</sub>θ

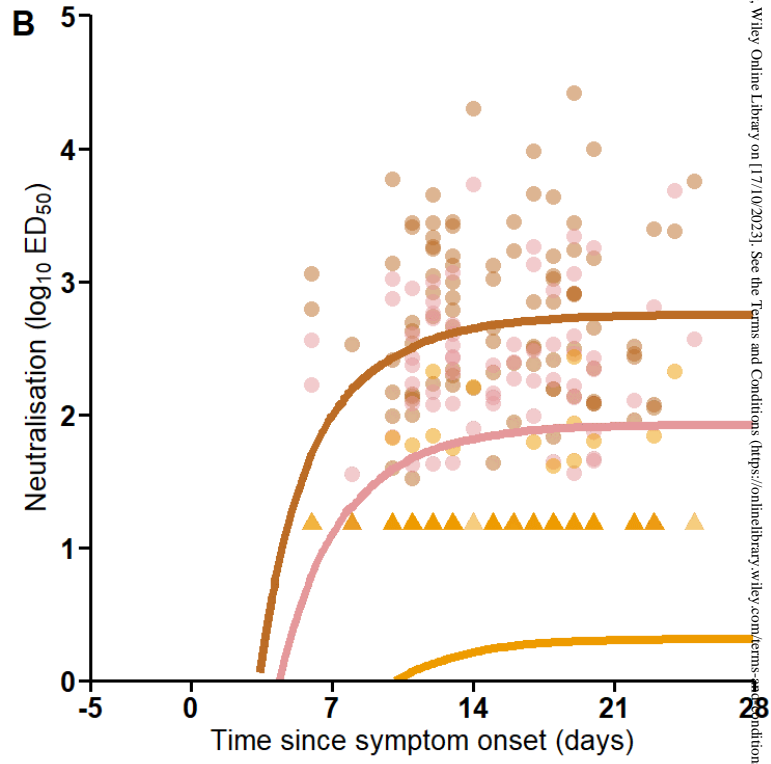
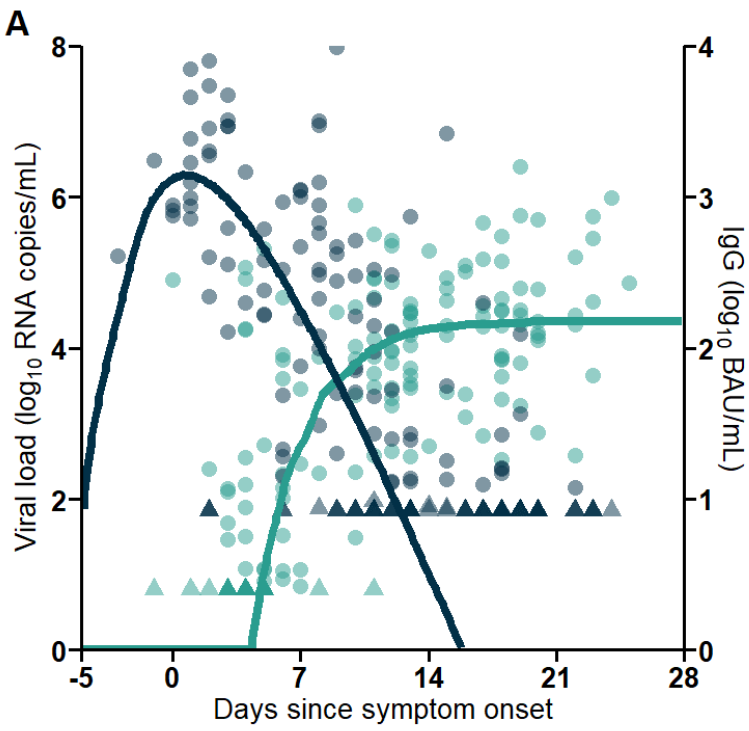
**Figure 3. Prediction of peak viral load distribution depending on ED<sub>50</sub> levels at initiation of infection.** Values of ED<sub>50</sub> : Pink: 0 ; Yellow: 10 ; Green: 100 ; Blue : 1000 ; Purple : 10000 ; Red : 100000

## SUPPORTING INFORMATION

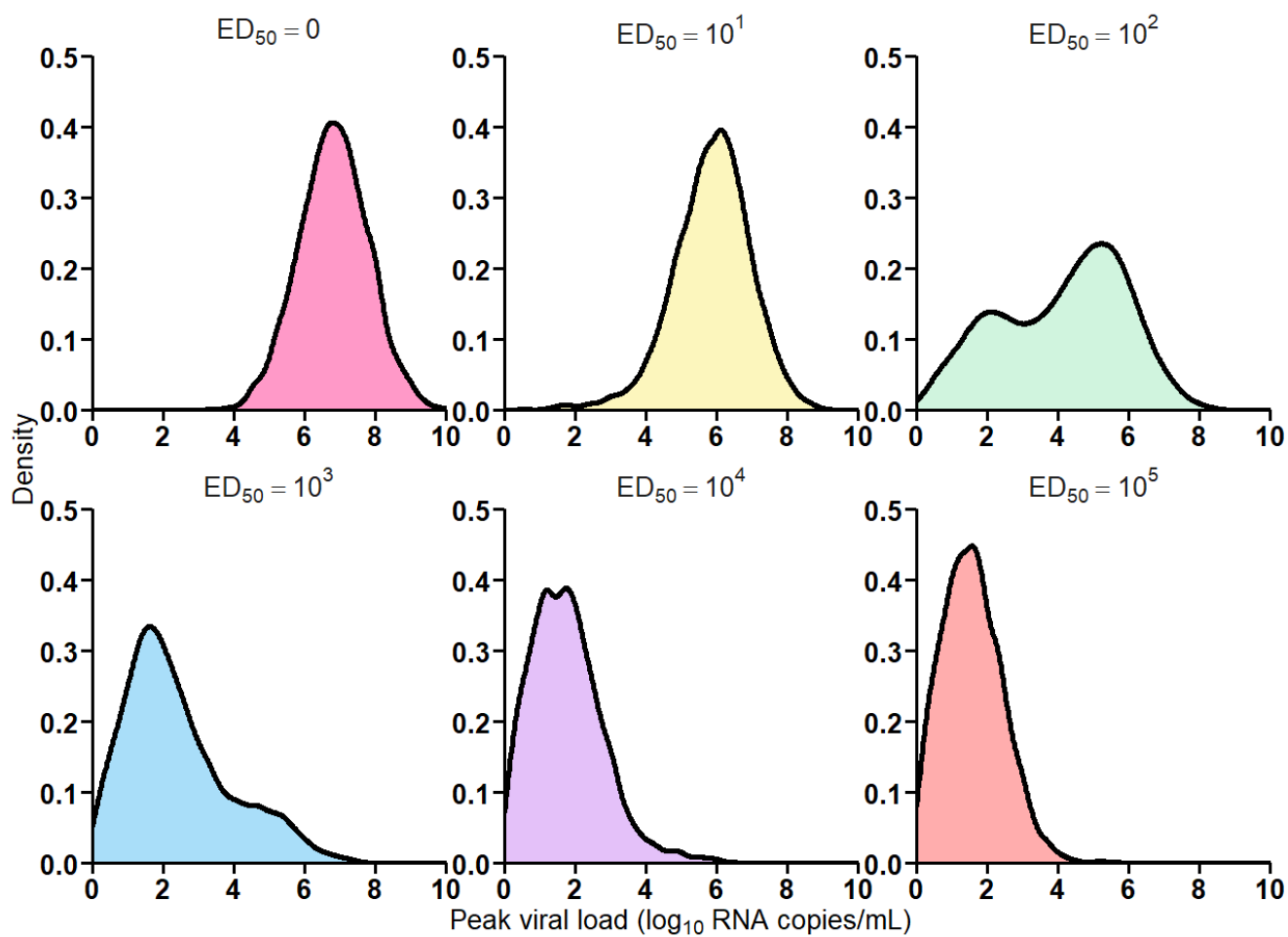
Supplementary information accompanies this paper on the *Clinical Pharmacology & Therapeutics* website ([www.cpt-journal.com](http://www.cpt-journal.com)).



2023-0439-f01-z-.tif



2023-0439-f02-z-.tif



2023-0439-f03-z.tif